# Radio polarimetry of Galactic Centre pulsars

D. H. F. M. Schnitzeler, R. P. Eatough, K. Ferrière, M. Kramer, K. J. Lee, A. Noutsos, R. M. Shannon

# Radio polarimetry of Galactic Centre pulsars

D. H. F. M. Schnitzeler,[1]★ R. P. Eatough,[1] K. Ferrière,[2] M. Kramer,[1] K. J. Lee,[3] A. Noutsos[1] and R. M. Shannon[4,5]

[1]*Max Planck Institut für Radioastronomie, D-53121 Bonn, Germany*
[2]*IRAP, Université de Toulouse, CNRS, BP 44346, F-31028 Toulouse Cedex 4, France*
[3]*Kavli Institute for Astronomy and Astrophysics, Peking University, Beijing 100871, People's Republic of China*
[4]*Australia Telescope National Facility, CSIRO Astronomy and Space Science, Marsfield, NSW 2122, Australia*
[5]*International Centre for Radio Astronomy Research (ICRAR), Curtin University, Bentley, WA 6102, Australia*

## ABSTRACT

To study the strength and structure of the magnetic field in the Galactic Centre (GC), we measured Faraday rotation of the radio emission of pulsars which are seen towards the GC. Three of these pulsars have the largest rotation measures (RMs) observed in any Galactic object with the exception of Sgr A⋆. Their large dispersion measures, RMs and the large RM variation between these pulsars and other known objects in the GC implies that the pulsars lie in the GC and are not merely seen in projection towards the GC. The large RMs of these pulsars indicate large line-of-sight magnetic field components between ∼16 and 33 μG; combined with recent model predictions for the strength of the magnetic field in the GC this implies that the large-scale magnetic field has a very small inclination angle with respect to the plane of the sky (∼12°). Foreground objects like the Radio Arc or possibly an ablated, ionized halo around the molecular cloud G0.11-0.11 could contribute to the large RMs of two of the pulsars. If these pulsars lie behind the Radio Arc or G0.11-0.11 then this proves that low-scattering corridors with lengths ≳100 pc must exist in the GC. This also suggests that future, sensitive observations will be able to detect additional pulsars in the GC. Finally, we show that the GC component in our most accurate electron density model oversimplifies structure in the GC.

**Key words:** pulsars: individual: PSR J1746−2849 – pulsars: individual: PSR J1745−2900 – pulsars: individual: PSR J1746−2856 – pulsars: individual: PSR J1745−2912 – ISM: magnetic fields – Galaxy: centre.

## 1 INTRODUCTION

The distribution of ionized gas and the strength and structure of the magnetic field in the Galactic Centre (GC)[1] have been probed using diffuse synchrotron emission (e.g. Yusef-Zadeh, Morris & Chance 1984; Tsuboi et al. 1986, and Sofue et al. 1987) and extragalactic radio sources (Roy, Pramesh Rao & Subrahmanyan 2008). These early measurements found evidence for strong magnetic fields, dense gas, and a new phenomenon: non-thermal radio filaments (NTFs), which are thin strands or sheets of synchrotron-emitting plasma. Over the last few decades many new insights have shed light on this complex environment, but important questions regarding the strength and structure of the magnetic field that pervades the GC remain unanswered (for a critical review see Ferrière 2011).
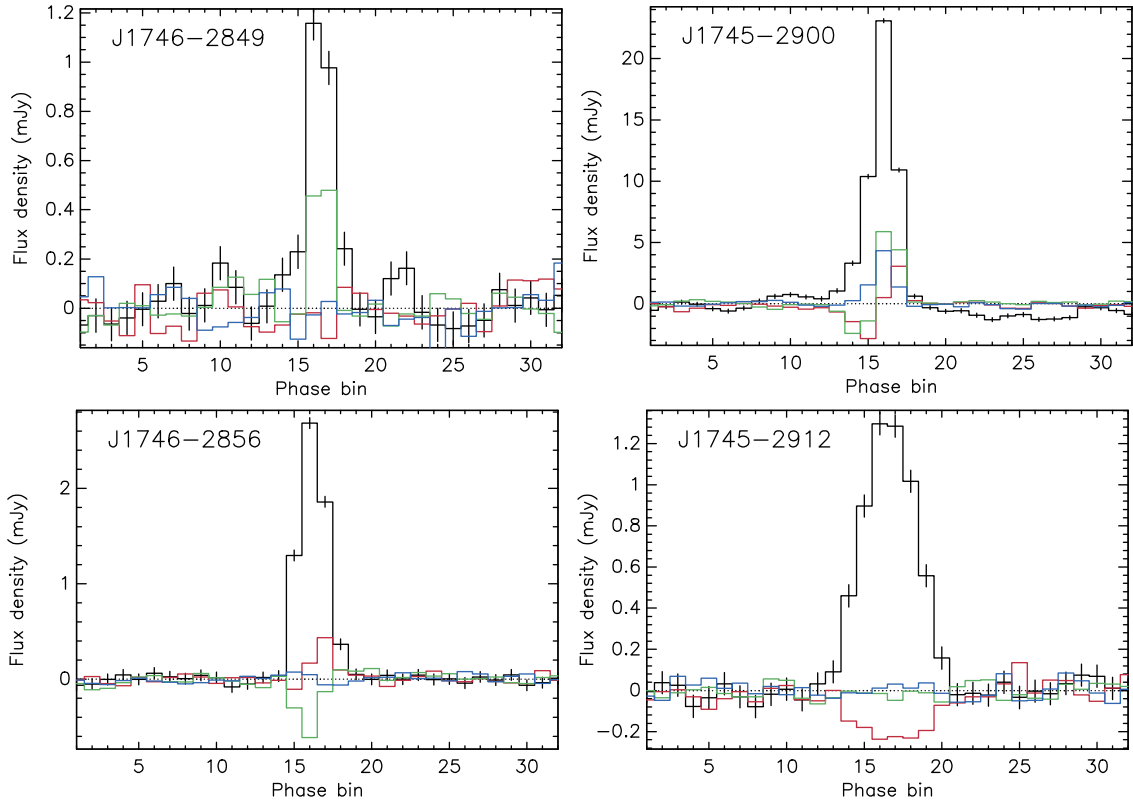
We study the properties of the magnetic field in the GC by observing all known radio pulsars within ≈20 arcmin of Sgr A⋆. First, we establish that these pulsars lie in the GC and are not merely seen towards it, then we investigate the implications for scattering in the GC. Radio pulsars have several advantages over source types that have been used previously: pulsars are perfect point sources, pulsar rotation measures (RMs) are produced exclusively in the Galactic foreground (Noutsos et al. 2009), pulsar distances can be estimated from the delay in pulse arrival times with frequency (quantified by the dispersion measure DM), and the line-of-sight (LOS) magnetic field component in the interstellar medium (ISM) can be estimated from the amount of Faraday rotation of the pulsar signal (quantified by RM). At a wavelength $\lambda$, the amount of Faraday rotation is equal to $\chi - \chi_0 = \mathrm{RM}\,\lambda^2$, where $\chi$ and $\chi_0$ are the observed and the intrinsic polarization angle of the emission, respectively,

$$\mathrm{RM}\ (\mathrm{rad\ m^{-2}})\ =\ 0.81 \int_{\mathrm{source}}^{\mathrm{observer}} n_{\mathrm{e}} B_{\parallel}\,\mathrm{d}l, \qquad (1)$$

where $n_{\mathrm{e}}$ is the local electron density in units of $\mathrm{cm^{-3}}$, $B_{\parallel}$ the LOS component of the magnetic field in units of $\mu$G, and the path length

★E-mail: schnitzeler@mpifr-bonn.mpg.de

[1] Throughout this paper, we will refer to the inner ∼150 pc region centred on Sgr A⋆ as 'the GC', which corresponds to the region with strongly enhanced electron densities in NE2001 (Cordes & Lazio 2002).

**Figure 1.** Pulse profiles of the target pulsars, showing Stokes *I* (black), *Q* (red) and *U* (green) after correcting for Faraday rotation using the RMs from Table 1, and *V* (blue). The Stokes *I* profile also shows $1\sigma$ errors.

*l* is measured in parsec. If the LOS component of the magnetic field points towards us $B_\parallel$ is positive, RM increases, and the plane of polarization is rotated counterclockwise. The dispersion measure DM is defined as

$$\text{DM}\left(\text{cm}^{-3}\,\text{pc}\right) = \int_{\text{source}}^{\text{observer}} n_e \mathrm{d}l\,, \qquad (2)$$

and the emission measure EM $\left(\text{cm}^{-6}\,\text{pc}\right) = \int_{\text{source}}^{\text{observer}} n_e^2 \mathrm{d}l$. The pulsars in our sample have been discovered by Johnston et al. (2006) and Deneva, Cordes & Lazio (2009) and include also the recently discovered magnetar PSR J1745−2900 which is known to lie close to Sgr A*(Eatough et al. 2013; Kennea et al. 2013; Mori et al. 2013; Shannon & Johnston 2013).

This paper is structured as follows: in Section 2, we describe the observations and their calibration, and in Section 3 we interpret our results in terms of the structure of the magnetized ISM in the GC. In Section 4, we summarize our results. We will adopt a distance of 8.3 kpc to the GC (Reid et al. 2014); at this distance 1 arcmin on the sky corresponds to a distance of 2.4 parsec.

## 2 OBSERVATIONS

The targets were observed with the Australia Telescope Compact Array (ATCA) in the 6A configuration between the 20th and the 22nd of April, and on the 6th of May 2015. These observations cover the frequency range between 4.473 and 6.525 GHz with 513 channels that are 4 MHz wide. PSR J1745−2900 was observed for 2.6 h in total, other targets were observed for 5.1 h each. Because of telescope maintenance all six antennas were only available on the final observing run. On the first three observing runs only 4, 5, and 4 antennas, respectively, were available. We calibrated the data

using the MIRIAD software package (Sault, Teuben & Wright 1995): PKS 1934−638 was used to determine the bandpass and absolute flux scale, and PKS 1814−254 (9° from the targets) was observed approximately every 18 min to calibrate the complex gains and polarization leakages. We then transferred the calibration solutions to the target pulsars, and flagged radio frequency interference. PKS 1814−254 rises after the target pulsars; therefore, the calibration solution from PKS 1814−254 was copied to the first observation of each target without extrapolation over time. In our analysis, we excluded the two shortest baselines.

Often the pulsar positions listed in the discovery papers had much larger errors than the size of the synthesized beam of our observations (≈4 arcsec × 1.5 arcsec), and we had to search maps of the primary beam to identify the pulsars. We removed a baseline level, calculated from off-pulse bins, before combining the real parts of the visibilities of the four observing runs using the noise variance in Stokes *V* as weights. Noise-weighted pulse profiles are shown in Fig. 1, and Table 1 lists the pulsars that we detected with the ATCA, their updated coordinates, and the peak total intensity. Positions were determined after summing the two brightest phase bins from the data collected in 2015 May.

The pulsars listed in Table 1 are bright enough that we could detect them in our most sensitive observing run. We were not able to detect PSR J1746−2850, even after concatenating visibilities – across all possible pulse phase bin combinations – from our two most sensitive observing runs,[2] giving a 6σ limit on the peak flux density of 0.49 mJy. This non-detection implies that the flux density

---

[2] The ATCA depends on pulsar ephemerides to generate pulse profiles; it is not possible to record baseband or pulsar search data. Although we used the most recent available ephemerides, the non-detection of PSR J1746−2850

**Table 1.** Properties of the pulsars that we detected: Coordinates (Equatorial and Galactic), DM, Stokes $I$ flux density of the brightest phase bin, polarized flux density and intrinsic polarization angle at 5.5 GHz ($\chi_0 = 0°$ towards the west and increases counter-clockwise), flux spectral index $\alpha$, and RM. For comparison, the Galactic coordinates of Sgr A⋆ are gl, gb = $-0°056$, $-0°046$ (Reid et al. 1999). $\chi_4^2$ lists the value of the chi-square statistic for four degrees of freedom, while 'S/N' indicates the signal/noise level of a 1D Gaussian random variable which produces the same probability.

| | J1746−2849 | J1745−2900 | J1746−2856 | J1745−2912 |
|---|---|---|---|---|
| RA(2000) | $17^h46^m03^s355(8)$ | $17^h45^m40^s16^b$ | $17^h46^m49^s856(3)$ | $17^h45^m47^s830(8)$ |
| Dec.(2000) | $-28°50'13''56(23)$ | $-29°00'29''82^b$ | $-28°56'59''23(10)$ | $-29°12'30''77(23)$ |
| gl | $0°134$ | $-0°056$ | $0°126$ | $-0°212$ |
| gb | $-0°030$ | $-0°047$ | $-0°233$ | $-0°175$ |
| DM (cm$^{-3}$pc)$^a$ | 1456 (D09) | 1778 (E13) | 1168 (J06) | 1130 (J06) |
| $I$ (mJy) | 1.16(7) | 23.08(17) | 2.68(6) | 1.30(5) |
| $PI_{5.5}$ (mJy) | 0.48(6) | 5.92(17) | 0.54(4) | 0.22(3) |
| $\chi_{0,\,5.5}$ (°) | 46.3(35) | 42.5(8) | 37.3(22) | −84.3(39) |
| $\alpha$ | −0.48(116) | 1.34(28) | −2.18(74) | −3.58(140) |
| RM (rad m$^{-2}$) | 10 104(101) | −66 080(24) | 13 253(53) | −535(107) |
| $\chi_4^2$ ('S/N') | 64 (7) | 779 (> 10) | 166 (> 10) | 54 (6) |

$^a$DM values were taken from Johnston et al. (2006, 'J06'), Deneva et al. (2009, 'D09'), and Eatough et al. (2013, 'E13').
$^b$Coordinates from Shannon & Johnston (2013).

of this source has decreased by at least a factor of 30 since it was discovered by Deneva et al. Radio magnetars are known to exhibit large variations in flux density (e.g. Lazaridis et al. 2008); if PSR J1746−2850 shares characteristics with radio magnetars, as was proposed by Deneva et al., then this could explain our non-detection. Monitoring observations might be able to detect this source in case it brightens again in the future. We excluded PSR J1745−2910 from our analysis because of its poorly constrained position and pulse period.

We determined the polarization properties of the pulsars using a new maximum-likelihood-based method that we developed, which we describe in a forthcoming paper (Schnitzeler et al., in preparation). In our method, the pulsar is characterized by its polarized flux density and intrinsic polarization angle at 5.5 GHz, its flux spectral index $\alpha$ ($S_\nu \propto \nu^\alpha$) and RM, plus, we allow the noise variances to be off by a scale factor $\eta$. Assuming that the differences between the measurements of Stokes $Q$ and $U$ and the model are described by Gaussian random variables and that the $N_{ch}$ frequency channels are independent, we maximize the log likelihood over the parameter space. We search for RMs out to $\pm 4 \times 10^5$ rad m$^{-2}$, the equivalent of the 'maximum RM' from Brentjens & de Bruyn (2005) in RM synthesis,[3] and $\alpha$ between −6 and 2, which covers all pulsar spectral indices that were determined by Lorimer et al. (1995) and Bates, Lorimer & Verbiest (2013). The difference between the maximum log likelihood and the log likelihood in the absence of any signal follows a chi square distribution (Wilks 1938) with in our case four degrees of freedom; this enables us to quantify the detection probability of each pulsar. The 68 per cent confidence limits for the pulsar parameters are based on the region where the log likelihood has decreased by 0.5 (e.g. Avni 1976).

Fig. 2 shows measured and modelled frequency spectra for the target pulsars, and our maximum likelihood estimates of the

could also indicate that the ephemeris for this pulsar was no longer accurate enough to fold the data correctly.
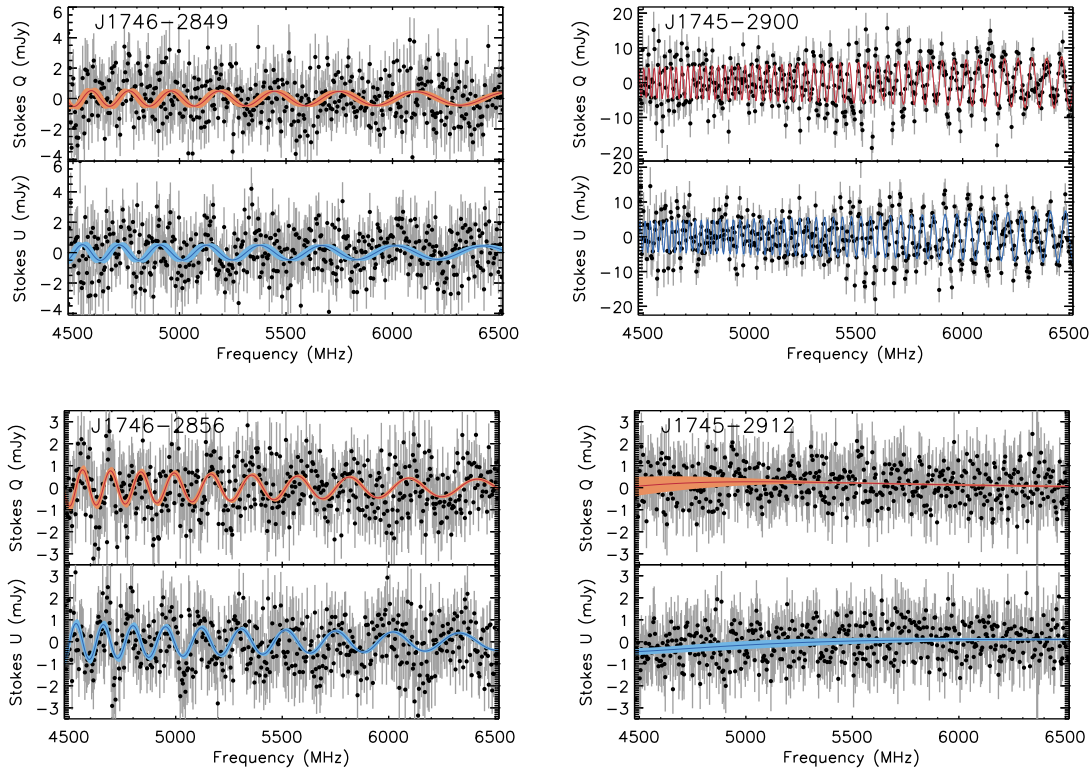[3] Introducing $\delta\lambda^2$ for the channel width in units of wavelength squared, the 'maximum RM' satisfies the equation RM$_{max}\delta\lambda^2 \approx \sqrt{3}$, even though RM synthesis assumes that for all frequency channels RM$\delta\lambda^2 \ll 1$ (both expressions are from Brentjens & de Bruyn 2005). The difference between the exact formalism by Schnitzeler & Lee (2015) and the formalism by Brentjens & de Bruyn (2005) is small for our observing setup and the RM range that we chose.

polarization properties of each pulsar are listed in Table 1. Fig. 3 shows the positions of the pulsars relative to other features in the GC. Scintillation of PSR J1745−2900 leads to a systematic and statistically significant variation between the amplitudes of the observed and modelled spectra across the frequency band. To increase the signal strength in our maximum likelihood estimation, we summed the polarization vectors of the brightest two phase bins in the pulse profile of PSR J1746−2856 and PSR J1746−2849, while for PSR J1745−2912 we summed the brightest four phase bins. If the intrinsic polarization angle $\chi_0$ changes across the pulse profile, this leads to depolarization if the polarization vectors of different phase bins are added. To mitigate this effect, we added a phase gradient to the polarization vectors of the different phase bins before summing the bins. We varied the gradient between 0°/bin and 180°/bin, and used the gradient which produced the strongest polarized signal. The largest phase gradient is 29°/bin.

## 3 DISCUSSION

The large DMs suggest that all target pulsars lie within ≈150 pc of Sgr A⋆ (based on the free electron density models NE2001 and NE2001thick; Cordes & Lazio 2002; Schnitzeler 2012), within the Central Molecular Zone and the footprint of the GC Lobe (Sofue & Handa 1984). Johnston et al. (2006) and Deneva et al. (2009) noticed that the pulse broadening times of the pulsars in our sample are much shorter than predicted by these electron density models. The absence of strong scattering does not preclude these pulsars from being in the GC: as shown by Lazio et al. (1999), Bower, Backer & Sramek (2001), and Roy (2013), the observed scattering sizes of extragalactic sources within ≈1° of Sgr A⋆ can be more than an order of magnitude smaller than predicted by NE2001. PSRs J1746−2856 and J1746−2849 have the largest RMs measured for any object in the Milky Way beyond 0.1 pc of Sgr A⋆ (Bower et al. 2003; Marrone et al. 2007; Eatough et al. 2013); out of all known pulsars only PSR J1745−2900 has a larger RM. All NTFs have smaller RMs, and the RMs of almost all extragalactic sources seen towards the GC are an order of magnitude smaller.

To calculate pulsar distances, NE2001 assumes a smoothly varying distribution for $n_e$ which peaks at 10 cm$^{-3}$. However, there is evidence for large $n_e$ variations in the GC. Electron densities of several hundred cm$^{-3}$ have been measured with the *KAO*, VLA, and the *ISO* satellite (Colgan et al. 1996; Lang, Goss & Morris
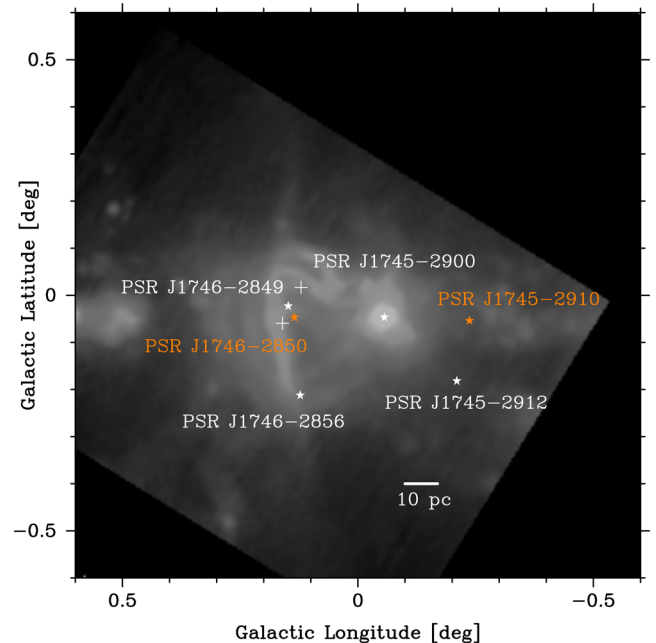
**Figure 2.** Frequency spectra of the target pulsars, showing Stokes $Q$ (top panel) and $U$ (bottom panel) together with the best-fitting models and 68 per cent confidence intervals.

2001; Rodríguez-Fernández, Martín-Pintado & de Vicente 2001; Cotera et al. 2005). Each sightline through the GC is thought to pass through at least one molecular cloud (Bally et al. 1988); because molecular cloud cores[4] are not significantly ionized, clouds leave holes in the $n_e$ distribution with typical diameters of up to 20 pc (full width at half-maximum; this value is based on the median diameter of molecular clouds in the CO survey by Oka et al. 2001). Simpson et al. (2007) derived EMs along a strip at a Galactic longitude of $\approx 0°.11$, and the $n_e$ values they calculated vary by more than an order of magnitude. Finally, the amount of diffuse radio emission at 10.55 GHz (Fig. 3) varies strongly with position, which could point to variations in the amount of free–free emission and therefore to variations in $n_e$. These results demonstrate that large $n_e$ variations exist in the GC. Therefore, one may not rely on the difference between the DMs of two pulsars to estimate their relative LOS positions.

Uchida, Sofue & Shibata (1985) predicted that winding up of field lines due to differential rotation in the GC leads to an outflow perpendicular to the Galactic plane, and produces a checkerboard pattern in RM centred on Sgr A⋆ (fig. 3 in Novak et al. 2003 and fig. 14 in Law, Brentjens & Novak 2011). As discussed by Novak



**Figure 3.** Known GC pulsars overplotted on an Effelsberg single-dish total intensity map of the GC at 10.55 GHz (Seiradakis et al. 1989). The positions of the Quintuplet and Arches clusters are indicated with pluses, and pulsars that we did not detect are highlighted in orange. On this scale, PSR J1745−2900 and Sgr A⋆ lie in the same direction.

[4] Lazio et al. (1999) argue that the ionized edges of molecular clouds could explain why scattering in the GC is patchy. They assumed that gas with a density $n(H_2) \gtrsim 500\,\mathrm{cm}^{-3}$ is highly ionized, however, these layers of dense gas are surrounded by more tenuous gas that could shield the inner regions from ionizing radiation (e.g. Hollenbach & Tielens 1999). The role that molecular clouds play in the scattering of background sources could be investigated with radiative transfer models that include chemical networks, e.g. CLOUDY (Ferland et al. 2013).

et al. and Law et al.,[5] the signs of the RMs of NTFs agree with one of the two possible patterns. However, the signs of the RMs of PSRs J1745−2912 and J1746−2856 contradict the particular solution selected by Uchida et al. and by Novak et al. The sign of RM of PSR J1746−2849 agrees with the model prediction because this pulsar lies at a slightly higher Galactic latitude than Sgr A⋆ (Reid et al. 1999), but since this latitude difference is very small, the winding up of field lines along the LOS towards PSR J1746−2849 generates only a small RM. A large foreground RM could shift the centre of the RM pattern and disrupt the checkerboard pattern. However, the RMs of PSRs J1746−2856 and J1746−2849 are much larger in magnitude than the RMs of NTFs and extragalactic radio sources, which implies that the foreground contribution cannot explain the difference in sign between the RMs we observe and the RMs Uchida et al. predict.

The contribution by the Galactic foreground could dominate the RM of PSR J1745−2912, and because the RM of PSR J1745−2900 is dominated by the high $n_e$ and strong magnetic field close to Sgr A⋆ (Eatough et al. 2013), we exclude these two pulsars from our analysis. For the remaining two pulsars, we calculate $\langle B_\parallel \rangle$, the mean LOS component of the magnetic field, weighted with the free electron density:

$$\langle B_\parallel \rangle \equiv \frac{\int B_\parallel n_e \mathrm{d}l}{\int n_e \mathrm{d}l} = \frac{\mathrm{RM}}{0.81\,\mathrm{DM}} \, ,$$

using the definition of DM from equation (2). If $B_\parallel$ changes sign along the LOS then locally $|B_\parallel|$ will be larger than $|\langle B_\parallel \rangle|$. We subtract 670 cm$^{-3}$pc from the observed DMs to correct for the foreground contribution: this is the DM value predicted by NE2001 for the LOS towards PSR J1745−2900, integrating from the Sun out to 150 pc from Sgr A⋆.[6] The extragalactic sources that Roy et al. (2008) analysed show large variations in RM, which in large part could be produced by the Galactic foreground. Estimating the foreground RM from these observations is very difficult, and we did not correct the pulsar RMs for the foreground contribution. By not correcting for the foreground RM, which is perhaps as high as 1500 rad m$^{-2}$, we overestimate $|\langle B_\parallel \rangle|$ by $\lesssim$15 per cent. For PSR J1746−2856 $\langle B_\parallel \rangle = 33\,\mu$G, and for PSR J1746−2849 $\langle B_\parallel \rangle = 16\,\mu$G, which are both much higher than the strength of the ordered and turbulent magnetic field in the vicinity of the Sun (1.5–2 μG and 3–6 μG, respectively; e.g. Haverkorn 2015). Strong magnetic fields are not uncommon in the GC: in their analysis of the 'Snake' NTF, Gray et al. (1995) derived $\langle B_\parallel \rangle \approx 7\,\mu$G for the foreground ISM. LaRosa et al. (2005) analysed maps of the diffuse synchrotron emission in the GC, and showed using minimum-energy arguments that the magnetic field strength $B \simeq 6\,(k/f)^{2/7}\,\mu$G, where $k$ is the ratio of energies of cosmic ray protons and electrons, and $f$ the filling factor of the synchrotron-emitting gas. For reasonable values of $k$ and $f$, $B \simeq (6\text{–}80)\,\mu$G (Ferrière 2011). Since the $\langle B_\parallel \rangle$ we derive are lower limits to $B$, our measurements rule out the weakest pervasive fields that are allowed in the analysis by LaRosa et al. If a magnetic field with $B \sim 160\,\mu$G (Crocker et al. 2011) pervades the GC, including the warm ionized medium that is probed by our

measurements, then the small $|\langle B_\parallel \rangle|$ we derive for PSR J1746−2856 implies an angle ∼12° between the magnetic field vector and the plane of the sky; towards PSR J1746−2849, which lies closer to the Galactic plane, this angle is even smaller. If $B_\parallel$ changes sign along the LOS then locally the angle between the magnetic field and the plane of the sky can be larger than the values we derived.

PSRs J1746−2849 and J1746−2856 are seen in the direction of the Radio Arc NTF (Fig. 3), which is known to have RMs between −5500 and −1660 rad m$^{-2}$ ('Source A' at gl, gb = 0°.16, −0°.13; Sofue et al. 1987) and between −200 and 1000 rad m$^{-2}$ ('Source A'' at gl, gb = 0°.16, −0°.18; Sofue et al. 1987). The 'Plumes' are the northern and southern extension of the Radio Arc, and show RMs between −500 and 1000 rad m$^{-2}$ (northern plume) and between −1500 and 0 rad m$^{-2}$ (southern plume). The RMs for the Radio Arc and the Plumes have been published by Inoue et al. (1984), Sofue et al. (1987), Tsuboi et al. (1986), Yusef-Zadeh et al. (1986), and Yusef-Zadeh & Morris (1987). The large RM variations that we measured for the GC pulsars and between these pulsars and the different parts of the Radio Arc could be produced in the turbulent GC. Variations in RM by several thousand rad m$^{-2}$ on scales of arcminutes have also been observed towards NTFs (Gray et al. 1995; Yusef-Zadeh, Wardle & Parastaran 1997; Lang, Morris & Echevarria 1999; Lang et al. 1999). NTFs like the 'Pelican' and the 'Ripple' are known to have external Faraday screens, which implies that the observed variations in RM occur outside the NTF, in the ISM of the GC. Only the GC shows such large RM fluctuations, adding support that our pulsars are in the GC. This also strengthens the case for PSR J1745−2912 lying in the GC, because its DM is very similar to the DM of PSR J1746−2856. If PSRs J1746−2856 and J1746−2849 lie along low-scattering 'corridors' through the GC, this again raises the question why not more pulsars have been detected in the GC. To answer this question requires a more detailed study of the GC environment and its pulsar population, taking into account the various instrumental effects and selection biases (building on, e.g. Chennamangalam & Lorimer 2014).

We cannot exclude the possibility that a foreground object in the GC adds a large RM (∼10$^4$ rad m$^{-2}$) to PSRs J1746−2856 and J1746−2849. A helical magnetic field around the Radio Arc could be the origin of this RM, and might produce also the helical features in Stokes *I* around the Radio Arc that were identified by Yusef-Zadeh & Morris (1987). The molecular cloud G0.11-0.11 lies at gl, gb = 0°.108, −0°.108 (Tsuboi, Ukita & Handa 1997), in between PSRs J1746−2856 and J1746−2849. Ablated gas from this cloud which is subsequently ionized might be an alternative explanation for the large RMs of these pulsars. However, the inner part of G0.11-0.11 that emits in the CS $J = 1 \rightarrow 0$ line (which traces gas with densities $n(H_2) \gtrsim 10^4$ cm$^{-3}$; Bally et al. 1988) has a diameter of only 7 pc (Tsuboi et al. 1997), while the pulsars are separated by about 29 pc on the sky if they lie in the GC. Even though a transition region exists between the dense gas in the inner parts of G0.11-0.11 and the low-density environment of the cloud, the ionized halo surrounding G0.11-0.11 would have to be very large for it to contribute to the RMs of both pulsars. Both scenarios require that the pulsars lie behind the Radio Arc or G0.11-0.11, which places the pulsars at the distance of Sgr A⋆ (Ponti et al. 2010; Roy 2013). If correct, this provides further evidence that long (>100 pc), low-scattering corridors exist in the GC.

## 4 SUMMARY

We studied the properties of the magnetic field in the GC by measuring the amount of Faraday rotation in the signals of four pulsars

---

[5] Law et al. modelled the magnetized ISM in the GC using observations of polarized diffuse radio emission. However, diffuse radio emission originates not only in the GC; furthermore, it can suffer from a range of depolarization effects, as discussed by, e.g. Sokoloff et al. (1998). Because of these concerns, we prefer to compare our results to those presented by Uchida et al. and Novak et al.

[6] We noticed that along this LOS DMs do not increase monotonically with distance in NE2001.

in the GC. We observed these pulsars with the Australia Telescope Compact Array at frequencies between 4.5 and 6.5 GHz. Our measurements provide more accurate positions for three of the previously known pulsars in the GC. The non-detection of PSR J1746−2850 implies that the flux density of this pulsar has decreased by at least a factor of 30 since its discovery by Deneva et al. (2009). To include both the flux spectrum of each pulsar and the variation in sensitivity across the observing band, we used a new maximum-likelihood based method that we will describe in an upcoming paper. PSRs J1746−2856 and J1746−2849 have RMs $> 10^4$ rad m$^{-2}$, the second and third largest RMs measured for any pulsar after PSR J1745−2900, and the largest RM measured for any Galactic object beyond ∼0.1 pc of Sgr A⋆. Their DMs, RMs, and RM variations place these pulsars within ≈150 pc of Sgr A⋆, within the Central Molecular Zone and the footprint of the GC Lobe. Based on evidence from the literature, we could not pin-point the pulsar positions more accurately based on only their DMs; the smooth structure in the free electron density that is assumed in NE2001 is an oversimplification.

Differential rotation in the GC, leading to a winding-up of field lines, was predicted to produce a checkerboard pattern in the sign of RM (Uchida et al. 1985); the RMs of NTFs agreed with one of the two possible solutions for this pattern (e.g. Novak et al. 2003). However, the signs of the RMs of PSRs J1746−2856 and J1746−2849 contradict this particular solution. By combining the observed DMs and RMs, and correcting for the foreground contribution to DM, we derive LOS lengths of the magnetic field vector between ∼16 and 33 μG, which is much larger than the strength of the large-scale and small-scale magnetic field in the vicinity of the Sun (Haverkorn 2015). If the GC, including the warm ionized medium that is probed by our observations, is pervaded by a strong magnetic field, $B \sim 160$ μG (Crocker et al. 2011), then our measurements imply that the magnetic field makes an angle ≲12° with the plane of the sky. If the direction of the LOS magnetic field component changes sign along the LOS, this inclination angle will be larger. Large changes in RM on scales of arcminutes have been observed previously towards NTFs; since the GC is the only location where such large RM variations are known to exist, this provides additional evidence that the target pulsars must lie inside the GC. The large RMs of PSRs J1746−2856 and J1746−2849 could be produced by foreground objects such as the Radio Arc or an ablated, ionized halo that surrounds the molecular cloud G0.11-0.11. This implies that these two pulsars must lie close to or even beyond Sgr A⋆, more than 100 pc into the GC, which would be additional evidence for the existence of long, low-scattering corridors through the GC. If this is indeed the case, then future, sensitive observations should be able to detect more pulsars in the GC (e.g. Chennamangalam & Lorimer 2014; Eatough et al. 2015).

## REFERENCES

Avni Y., 1976, ApJ, 210, 642
Bally J., Stark A. A., Wilson R. W., Henkel C., 1988, ApJ, 324, 223

Bates S. D., Lorimer D. R., Verbiest J. P. W., 2013, MNRAS, 431, 1352
Bower G. C., Backer D. C., Sramek R. A., 2001, ApJ, 558, 127
Bower G. C., Wright M. C. H., Falcke H., Backer D. C., 2003, ApJ, 588, 331
Brentjens M. A., de Bruyn A. G., 2005, A&A, 441, 1217
Chennamangalam J., Lorimer D. R., 2014, MNRAS, 440, L86
Colgan S. W. J., Erickson E. F., Simpson J. P., Haas M. R., Morris M., 1996, ApJ, 470, 882
Cordes J. M., Lazio T. J. W., 2002, preprint (astro-ph/0207156)
Cotera A. S., Colgan S. W. J., Simpson J. P., Rubin R. H., 2005, ApJ, 622, 333
Crocker R. M., Jones D. I., Aharonian F., Law C. J., Melia F., Oka T., Ott J., 2011, MNRAS, 413, 763
Deneva J. S., Cordes J. M., Lazio T. J. W., 2009, ApJ, 702, L177
Eatough R. P. et al., 2013, Nature, 501, 391
Eatough R. et al., 2015, in Bourke et al., eds, Proc. Sci., Advancing Astrophysics with the Square Kilometre Array (AASKA14). SISSA, Trieste, PoS#331
Ferland G. J. et al., 2013, Rev. Mex. Astron. Astrofis., 49, 137
Ferrière K., 2011, in Morris M. R., Wang Q. D., Yuan F., eds, ASP Conf. Ser. Vol. 439, The Galactic Center: a Window to the Nuclear Environment of Disk Galaxies. Astron. Soc. Pac., San Francisco, p. 39
Gray A. D., Nicholls J., Ekers R. D., Cram L. E., 1995, ApJ, 448, 164
Haverkorn M., 2015, in Lazarian A., de Gouveia Dal Pino E. M., Melioli C., eds, Astrophysics and Space Science Library, Vol. 407, Magnetic Fields in Diffuse Media. Springer-Verlag, Berlin, p. 483
Hollenbach D. J., Tielens A. G. G. M., 1999, Rev. Mod. Phys., 71, 173
Inoue M., Takahashi T., Tabara H., Kato T., Tsuboi M., 1984, PASJ, 36, 633
Johnston S., Kramer M., Lorimer D. R., Lyne A. G., McLaughlin M., Klein B., Manchester R. N., 2006, MNRAS, 373, L6
Kennea J. A. et al., 2013, ApJ, 770, L24
Lang C. C., Anantharamaiah K. R., Kassim N. E., Lazio T. J. W., 1999, ApJ, 521, L41
Lang C. C., Morris M., Echevarria L., 1999, ApJ, 526, 727
Lang C. C., Goss W. M., Morris M., 2001, AJ, 121, 2681
LaRosa T. N., Brogan C. L., Shore S. N., Lazio T. J., Kassim N. E., Nord M. E., 2005, ApJ, 626, L23
Law C. J., Brentjens M. A., Novak G., 2011, ApJ, 731, 36
Lazaridis K., Jessner A., Kramer M., Stappers B. W., Lyne A. G., Jordan C. A., Serylak M., Zensus J. A., 2008, MNRAS, 390, 839
Lazio T. J. W., Anantharamaiah K. R., Goss W. M., Kassim N. E., Cordes J. M., 1999, ApJ, 515, 196
Lorimer D. R., Yates J. A., Lyne A. G., Gould D. M., 1995, MNRAS, 273, 411
Marrone D. P., Moran J. M., Zhao J.-H., Rao R., 2007, ApJ, 654, L57
Mori K. et al., 2013, ApJ, 770, L23
Noutsos A., Karastergiou A., Kramer M., Johnston S., Stappers B. W., 2009, MNRAS, 396, 1559
Novak G. et al., 2003, ApJ, 583, L83
Oka T., Hasegawa T., Sato F., Tsuboi M., Miyazaki A., Sugimoto M., 2001, ApJ, 562, 348
Ponti G., Terrier R., Goldwurm A., Belanger G., Trap G., 2010, ApJ, 714, 732
Reid M. J., Readhead A. C. S., Vermeulen R. C., Treuhaft R. N., 1999, ApJ, 524, 816
Reid M. J. et al., 2014, ApJ, 783, 130
Rodríguez-Fernández N. J., Martín-Pintado J., de Vicente P., 2001, A&A, 377, 631
Roy S., 2013, ApJ, 773, 67
Roy S., Pramesh Rao A., Subrahmanyan R., 2008, A&A, 478, 435
Sault R. J., Teuben P. J., Wright M. C. H., 1995, in Shaw R. A., Payne H. E., Hayes J. J. E., eds, ASP Conf. Ser. Vol. 77, Astronomical Data Analysis Software and Systems IV. Astron. Soc. Pac., San Francisco, p. 433
Schnitzeler D. H. F. M., 2012, MNRAS, 427, 664
Schnitzeler D. H. F. M., Lee K. J., 2015, MNRAS, 447, L26
Seiradakis J. H., Reich W., Wielebinski R., Lasenby A. N., Yusef-Zadeh F., 1989, A&AS, 81, 291
Shannon R. M., Johnston S., 2013, MNRAS, 435, L29

Simpson J. P., Colgan S. W. J., Cotera A. S., Erickson E. F., Hollenbach D. J., Kaufman M. J., Rubin R. H., 2007, ApJ, 670, 1115

Sofue Y., Handa T., 1984, Nature, 310, 568

Sofue Y., Reich W., Inoue M., Seiradakis J. H., 1987, PASJ, 39, 95

Sokoloff D. D., Bykov A. A., Shukurov A., Berkhuijsen E. M., Beck R., Poezd A. D., 1998, MNRAS, 299, 189

Tsuboi M., Inoue M., Handa T., Tabara H., Kato T., Sofue Y., Kaifu N., 1986, AJ, 92, 818

Tsuboi M., Ukita N., Handa T., 1997, ApJ, 481, 263

Uchida Y., Sofue Y., Shibata K., 1985, Nature, 317, 699

Wilks S. S., 1938, Ann. Math. Stat., 9, 60

Yusef-Zadeh F., Morris M., 1987, ApJ, 322, 721

Yusef-Zadeh F., Morris M., Chance D., 1984, Nature, 310, 557

Yusef-Zadeh F., Morris M., Slee O. B., Nelson G. J., 1986, ApJ, 310, 689

Yusef-Zadeh F., Wardle M., Parastaran P., 1997, ApJ, 475, L119

This paper has been typeset from a TEX/LATEX file prepared by the author.